The Tropical Tropopause Layer 1960–2100

A. Gettelman, T. Birner, V. Eyring, H. Akiyoshi, Slimane Bekki, C. Brühl, M. Dameris, D.E. Kinnison, Franck Lefèvre, F. Lott, et al.

Atmos. Chem. Phys., 9, 1621–1637, 2009
www.atmos-chem-phys.net/9/1621/2009/

Atmospheric Chemistry and Physics

The Tropical Tropopause Layer 1960–2100

A. Gettelman[1], T. Birner[2], V. Eyring[3], H. Akiyoshi[4], S. Bekki[6], C. Brühl[8], M. Dameris[3], D. E. Kinnison[1], F. Lefevre[6], F. Lott[7], E. Mancini[11], G. Pitari[11], D. A. Plummer[5], E. Rozanov[10], K. Shibata[9], A. Stenke[3], H. Struthers[12], and W. Tian[13]

[1]National Center for Atmospheric Research, Boulder, CO, USA
[2]University of Toronto, Toronto, ON, Canada
[3]Deutsches Zentrum für Luft- und Raumfahrt, Oberpfaffenhofen, Germany
[4]National Institute for Environmental Studies, Tsukuba, Japan
[5]Canadian Centre for Climate Modeling and Analysis, Victoria, BC, Canada
[6]Université Pierre and Marie Curie, Service d'Aeronomie, Paris, France
[7]L'Institut Pierre-Simon Laplace, Ecole Normale Superieur, Paris, France
[8]Max Planck Institut für Chemie, Mainz, Germany
[9]Meteorological Research Institute, Tsukuba, Japan
[10]Physikalisch-Meteorologisches Observatorium Davos, Davos, Switzerland
[11]Universita degli Studi de L'Aquila, L'Aquila, Italy
[12]National Institute for Water and Atmosphere, New Zealand
[13]University of Leeds, Leeds, UK

Received: 4 December 2007 – Published in Atmos. Chem. Phys. Discuss.: 29 January 2008
Revised: 23 January 2009 – Accepted: 23 January 2009 – Published: 4 March 2009

Abstract. The representation of the Tropical Tropopause Layer (TTL) in 13 different Chemistry Climate Models (CCMs) designed to represent the stratosphere is analyzed. Simulations for 1960–2005 and 1980–2100 are analyzed. Simulations for 1960–2005 are compared to reanalysis model output. CCMs are able to reproduce the basic structure of the TTL. There is a large (10 K) spread in annual mean tropical cold point tropopause temperatures. CCMs are able to reproduce historical trends in tropopause pressure obtained from reanalysis products. Simulated historical trends in cold point tropopause temperatures are not consistent across models or reanalyses. The pressure of both the tropical tropopause and the level of main convective outflow appear to have decreased (increased altitude) in historical runs as well as in reanalyses. Decreasing pressure trends in the tropical tropopause and level of main convective outflow are also seen in the future. Models consistently predict decreasing tropopause and convective outflow pressure, by several hPa/decade. Tropical cold point temperatures are projected to increase by 0.09 K/decade. Tropopause anomalies are highly correlated with tropical surface temperature anomalies and with tropopause level ozone anomalies, less so with stratospheric temperature anomalies. Simulated stratospheric water vapor at 90 hPa increases by up to 0.5–1 ppmv by 2100. The result is consistent with the simulated increase in temperature, highlighting the correlation of tropopause temperatures with stratospheric water vapor.

Correspondence to: A. Gettelman
(andrew@ucar.edu)

1 Introduction

The Tropical Tropopause Layer (TTL), the region in the tropics within which air has characteristics of both the troposphere and the stratosphere, is a critical part of the atmosphere. Representing the TTL region in global models is critical for being able to simulate the future of the TTL and the effects of TTL processes on climate and chemistry.

The TTL is the layer in the tropics between the level of main convective outflow and the cold point (see Sect. 2), about 12–18 km (Gettelman and Forster, 2002). The TTL has also been defined as a shallower layer between 15–18 km (see discussion in World Meteorological Organization (2007), Chapter 2). We will use the deeper definition of the TTL here because we seek to understand not just the

stratosphere, but the tropospheric processes that contribute to TTL structure (see below).

The TTL is maintained by the interaction of convective transport, convectively generated waves, radiation, cloud microphysics and the large scale stratospheric circulation. The TTL is the source region for most air entering the stratosphere, and therefore the chemical boundary conditions of the stratosphere are set in the TTL. Clouds in the TTL, both thin cirrus clouds and convective anvils, have a significant impact on the radiation balance and hence tropospheric climate (Stephens, 2005).

Changes to the tropopause and TTL may occur over long periods of time in response to anthropogenic forcing of the climate system. These trends are in addition to natural variability, which includes inter-annual variations such as the Quasi Biennial Oscillation (QBO, ∼2 years), the El Niño Southern Oscillation (ENSO, 3–5 years), the solar cycle (11 years), or transient variability forced by volcanic eruptions of absorbing and scattering aerosols. Changes in the thermal structure of the TTL may alter clouds, affecting global climate through water vapor and cloud feedbacks (Bony et al., 2006). Changes to TTL structure may alter transport (Fueglistaler and Haynes, 2005) and water vapor (Gettelman et al., 2001). TTL water vapor in turn may affect stratospheric chemistry, ozone (Gettelman and Kinnison, 2007) and water vapor, as well as surface climate (Forster and Shine, 2002). Changes in the Hadley circulation (Seidel et al., 2008) and the stratospheric Brewer-Dobson circulation (Butchart et al., 2006) may affect the meridional extent of the TTL. The changes may be manifest as changes to the mid-latitude storm tracks (Yin, 2005).

Several studies have attempted to look at changes to the tropopause and TTL over time. Seidel et al. (2001) found decreases in tropopause pressure (increasing height) trends in tropical radiosonde records. Gettelman and Forster (2002) described a climatology of the TTL, and looked at changes over the observed record from radiosondes, also finding decreases in tropopause pressure (increasing height) with little significant change in the bottom of the TTL (see below). Fueglistaler and Haynes (2005) showed that TTL trajectory analyses could reproduce changes in stratospheric entry water vapor. Santer et al. (2003) examined simulated changes in thermal tropopause height and found that they could only explain observations if anthropogenic forcings were included. Dameris et al. (2005) looked at simulations from 1960–1999 in a global model and found no consistent trend in thermal tropopause pressure or water vapor. Son et al. (2008) looked at changes to the global thermal tropopause pressure in global models and found a decrease (height increase) through the 21st century, less in models with ozone recovery.

Recently, Gettelman and Birner (2007), hereafter GB2007, have shown that two Coupled Chemistry Climate Models (CCMs), which are General Circulation Models (GCMs) with a chemistry package coupled to the radiation (so chemical changes affect radiation and climate), can reproduce key structural features of the TTL and their variability in space and time. GB2007 found that 2 models, the Canadian Middle Atmosphere Model (CMAM) and the Whole Atmosphere Community Climate Model (WACCM), were able to reproduce the structure of TTL temperatures, ozone and clouds. Variability from the annual cycle down to planetary wave time and space scales (days and 100 s km) was reproduced, with nearly identical standard deviations. There were significant differences in the treatment of clouds and convection between the two models, but this did not seem to alter the structure of the TTL. GB2007 conclude that CMAM and WACCM are able to reproduce important features of the TTL, and that these features must be largely regulated by the large scale structure, since different representations of subgrid scale processes (like convection) did not alter TTL structure or variability.

In this work, we will look at changes to the TTL over the recent past (1960–2005) and potential changes over the 21st century. We apply a similar set of diagnostics as GB2007 to WACCM, CMAM and 11 other CCMs that are part of a multi-model ensemble with forcings for the historical record (1960–2005), and using scenarios for the past and future (1980–2100). We will compare the models to observations over the observed record, and then examine model predictions for the evolution of the TTL in the 21st Century. These simulations have been used to assess future trends in stratospheric ozone in Eyring et al. (2007) and World Meteorological Organization (2007), Chapter 6. Trends are calculated only over periods when many or most models have output. We focus discussion on three questions: (1) Do tropospheric or stratospheric changes dominate at the cold point? (2) Does ozone significantly affect TTL structure? (3) What will happen to stratospheric water vapor?

The methodology, models, data and diagnostics are described in Sect. 2. The model climatologies are discussed in Sect. 3. Past and future trends from models and analysis systems are in Sect. 4. Discussion of some key issues is in Sect. 5 and conclusions are in Sect. 6.

2 Methodology

In this section we first describe the definition and diagnostics for the TTL (Sect. 2.1). We then briefly describe the models used and where further details, information and output can be obtained (Sect. 2.2). Finally we verify that using zonal monthly mean data provides a correct picture of the climatology and trends (Sect. 2.3).

2.1 Diagnostics

To define the TTL we focus on the vertical temperature structure, and we adopt the TTL definition of Gettelman and Forster (2002), also used in GB2007, as the layer between the level of maximum convective outflow and the cold

point tropopause (CPT). We also calculate the Lapse Rate Tropopause (LRT) for comparison and for analysis of the subtropics. The LRT is defined using the standard definition of the lowest point where the lapse rate is less than 2 K km^{-1} for 2 km ($-dT/dz$<2 K km^{-1}). The bottom of the TTL is defined as the level of maximum convective outflow. Practically, as shown by Gettelman and Forster (2002) the maximum convective outflow is where the potential temperature Lapse Rate Minimum (LRM) is located (the minimum in $d\theta/dz$), and it is near the Minimum Ozone level.

The TTL definition above is not the only possible one, but conceptually marks the boundary between which air is generally tropospheric (below) and stratospheric (above). The definition is convenient because the TTL can be diagnosed locally from a temperature sounding, and facilitates comparisons with observations.

We also examine the Zero Lapse Rate level (ZLR). The ZLR can be thought of as an interpolated CPT. The ZLR is defined in the same way as the lapse rate tropopause, except stating that instead of the threshold of -2 K km^{-1}, it is 0 K km^{-1}. It is the lowest point (in altitude) where the lapse rate is less than 0 K km^{-1} for 2 km ($-dT/dz$<0 K km^{-1}). As the lapse rate changes from negative (troposphere) to positive (stratosphere) it will have a value of zero at some intermediate location. The ZLR can be found by interpolation, so the ZLR is just a way to interpolate the temperature sounding to find the cold point instead of forcing the cold point to be at a defined level. The ZLR is found as for the LRT by taking the derivative of the temperature profile and interpolating to find the ZLR point. For the zonal monthly mean data available for this study the ZLR can capture changes to the thermal structure not seen in the CPT level. The CPT is defined to be a model level, while the ZLR can be interpolated like the LRT. It also serves as a check on the CPT. In general we find agreement between $P_{\rm ZLR}$ and $P_{\rm LRT}$ to within 10 hPa, and strong correlation in their variability. Table 1 provides a list of these abbreviations. For a schematic diagram, see Gettelman and Forster (2002), Fig. 11. Average locations of these levels are also shown in GB2007, Fig. 2.

2.2 Models

This work uses model simulations developed for the Chemistry Climate Model Validation (CCMVal) activity for the Stratospheric Processes and Their Role in Climate (SPARC) project of the World Climate Research Program (WCRP). The work draws upon simulations defined by CCMVal in support of the Scientific Assessment of Ozone Depletion: 2006 (World Meteorological Organization, 2007). There are two sets of simulations used. The historical simulation REF1 is a transient run from 1960 or 1980 to 2005 and was designed to reproduce the well-observed period of the last 25 years. All models use observed sea-surface temperatures, and include observed halogens and greenhouse gases. Some models include volcanic eruptions. Details of the forcings are described by Eyring et al. (2006), but are described here as they impact the results.

An assessment of temperature, trace species and ozone in the simulations of the thirteen CCMs participating here was presented in Eyring et al. (2006). Scenarios for the future are denoted "REF2" and are analyzed from 1960 or 1980 to 2050 or 2100 (as available). These simulations are described in more detail by Eyring et al. (2007), who projected the future evolution of stratospheric ozone in the 21st century from the 13 CCMs used here. Table 2 lists the model names, horizontal resolution and references, while details on the CCMs can be found in Eyring et al. (2006, 2007) and references therein. For the MRI and ULAQ CCMs the simulations used in Eyring et al. (2006, 2007) have been replaced with simulations from updated model configurations as the previous runs included weaknesses in the TTL.

Our purpose is not so much to evaluate individual models, but to look for consistent climatology and trends across the models. Details of individual model performance are contained in Eyring et al. (2006). We do however have high confidence in the present day TTL climatologies (mean and variability) of CMAM and WACCM, based on our more detailed analysis and detailed comparisons to observations in GB2007. We first will analyze model representation of the recent past to see if the models reproduce TTL diagnostics from observations. The analysis provides some insight into the confidence we might place in future projections. We will have more confidence of future projections for those diagnostics that (1) have consistent trends between models and (2) trends which match observations for the past.

Model output was archived at the British Atmospheric Data Center (BADC), and is used under the CCMVal data protocol. For more information obtaining the data, consult the CCMVal project (http://www.pa.op.dlr.de/CCMVal). The analysis from 11 models is conducted on monthly zonal mean output on standard pressure levels. In the TTL these levels are 500, 400, 300, 250, 200, 170, 150, 130, 115, 100, 90, 80 and 70 hPa. In Sect. 2.3 below we describe the implications of using monthly zonal means for calculating diagnostics rather than full 3-D fields.

For comparison with model output for the historical "REF1" runs, we use model output from the National Centers for Environmental Prediction/National Center for Atmospheric Research (NCEP/NCAR) Reanalysis Project (Kalnay et al., 1996), and the European Center for Medium rage Weather Forecasting (ECMWF) 40 year reanalysis "ERA40" (Uppala et al., 2005). Both are analyzed on 23 standard levels (i.e. 300, 250, 150, 100, 70 for TTL analyses). Because of significant uncertainties in trend calculations due to changes in input data records, we restrict our use of the NCEP/NCAR and ERA40 reanalysis data to the period from 1979–2001, when satellite temperature data is input for the reanalyses (and both ERA40 and NCEP have analyses). Even for the 1979–2001 period, analyses diverge between them for some

Table 1. Diagnostic Abbreviations used in the text

Abbreviation	Name
CPT	Cold Point Tropopause (at model levels)
ZLR	Zero Lapse Rate (interpolated $-dT/dz$<0 K km^{-1})
LRT	Lapse Rate Tropopause (interpolated $-dT/dz$¡2 K km^{-1})
LRM	Lapse Rate Minimum (interpolated $d\theta/dz$ minimum)

Table 2. CCMs Used in this study. Abbreviations for Institutions: Geophysical Fluid Dynamics Laboratory (GFDL), National Institute for Environmental Studies (NIES), Deutsches Zentrum für Luft- und Raumfahrt (DLR), National Aeronautics and Space Administration – Goddard Space Flight Center (NASA-GSFC), L'Institut Pierre-Simon Laplace (IPSL), Max Planck Institute (MPI), Meteorological Research Institute (MRI), Physikalisch-Meteorologisches Observatorium Davos (PMOD), Eidgenössische Technische Hochschule Zürich (ETHZ), National Center for Atmospheric Research (NCAR).

Model	Horizontal Resolution	TTL Vertical Res (km)	Institution	Reference
AMTRAC	2°×2.5°	1.5	GFDL, USA	Austin and Wilson (2006); Austin et al. (2007)
CCSRNIES	2.8°×2.8°	1.1	NIES, Japan	Akiyoshi et al. (2004); Kurokawa et al. (2005)
CMAM	3.75°×3.75°	1.1	Univ. Toronto, York Univ. Canada,	Beagley et al. (1997); de Grandpré et al. (2000)
E39C	3.75°×3.75°	0.7	DLR, Germany	Dameris et al. (2005, 2006)
GEOSCCM	2°×2.5°	1.0	NASA/GSFC, USA	Bloom et al. (2005); Stolarski et al. (2006)
LMDZrepro	2°×2.5°	1.0	IPSL, France	Lott et al. (2005); Jourdain et al. (2007)
MAECHAM4	3.75°×3.75°	1.5	MPI Met & MPI Chem. Germany,	Manzini et al. (2003); Steil et al. (2003)
MRI	2.8°×2.8°	0.5	MRI, Japan	Shibata and Deushi (2005); Shibata et al. (2005)
SOCOL	3.75°×3.75°	0.7	PMOD & ETHZ, Switzerland	Egorova et al. (2005); Rozanov et al. (2005)
ULAQ	10°×22.5°	2.5	Univ. L'Aquila, Italy	Pitari et al. (2002)
UMETRAC	2.5°×3.75°	1.5	Met Office, UK	Austin (2002); Austin and Butchart (2003) Struthers et al. (2004)
UMSLIMCAT	2.5°×3.75°	1.5	Univ. Leeds, UK	Tian and Chipperfield (2005)
WACCM	4°×5°	1.1	NCAR, USA	Garcia et al. (2007)

diagnostics. The difference is one indication of where systematic uncertainties lie.

There are known and significant problems with estimating tropopause trends from both the NCEP and ERA40 reanalyses due to data inhomogeneities and other sources. So we also include comparisons with a carefully selected radiosonde archive (Seidel and Randel, 2006) for P_{LRT}, T_{LRT}, P_{CPT}, T_{CPT} and P_{LRM}. Data were converted from monthly to annual anomalies by linear averages. For purposes of display, we have added the ERA40 mean to these anomalies on the plots.

Trends are calculated from annual diagnostic values using a bootstrap fit (Efron and Tibshirani, 1993). The bootstrap fitting procedure yields a standard deviation (σ) of the linear trend slope, which can be used to estimate the uncertainty. For calculations here we report the 2σ (95%) confidence interval. For multi-model ensembles we generate annual anomaly time series from each model. We take the mean of these annual anomalies for each year from all models, and then add back in the multi-model mean. The trend is calculated on the ensemble mean time-series using a bootstrap fit and a 2σ (95%) confidence interval for significance of the multi-model mean. The method described above is nearly the same as the method used by Solomon et al. (2007) in estimating multi-model ensemble differences and trends. Note that for almost all cases the mean of individual model trends is almost identical to the multi-model ensemble trend. We also use multiple linear regression to explore relationships between TTL diagnostics and surface temperature, stratospheric temperature and ozone at various levels.

2.3 Analysis

Zonal monthly mean output on a standard set of levels (see Sect. 2.2 and Fig. 3), is available from most CCMs. In this section we show that use of zonal monthly mean temperatures and ozone on these standard levels to calculate TTL diagnostics has only minor affects on the results of the analysis

to be presented in Sects. 3 and 4 below, and does not significantly impact the conclusions.

In general a diagnostic calculated from an average of individual profiles is not equal to the average of the diagnostic calculated for each profile. For example, in the case of the LRT interpolation to standard levels and monthly and zonal averaging of a model temperature field is involved, and the averaging may affect the results. However, we do have 3-D instantaneous model output available from WACCM and CMAM for comparison to verify that the averaging does not affect the results. Differences between 2-D and 3-D output have also been discussed by Son et al. (2008) for global tropopause height trends using a subset of model runs in this study.

Figure 1 shows (A) WACCM January zonal mean Cold Point Tropopause Temperature (T_{CPT}), (B) Lapse Rate Tropopause Pressure (P_{LRT}) and (C) Lapse Rate Minimum pressure (P_{LRM}) from 3-D instantaneous profiles (black) and from monthly zonal mean output (gray) for 60 S–60 N latitude. The thin lines are $\pm 2\sigma$ in the 3-D model output. The monthly zonal mean cold point and lapse rate minimum are reproduced, within 1 K (T_{CPT}) and 10 hPa (P_{LRM}) in the tropics, and within the $\pm 2\sigma$ (95%) variability (Fig. 1a and b). The P_{LRM} is also reproduced in the tropics to within one model level and within the 2σ variability of the 3-D model output (Fig. 1c). Since the P_{LRM} is a level and not interpolated, a single monthly mean value has a coarse distribution dependent on standard pressure levels. A plot of P_{LRM} like Fig. 1 for CMAM also shows agreement between zonally averaged and 3-D output within the range of model variability. Results for other months yield the same conclusions for WACCM and CMAM.

GB2007 analyzed models with much higher (0.3 km) vertical resolution and 1.1 km vertical resolution, and obtained TTL structures that were not qualitatively different. The lapse rate and cold point tropopause, the level of zero radiative heating, the minimum ozone level and the minimum lapse rate level were all in approximately the same location, and the same location relative to each other, with about the same variability. Thus we do not think the model vertical resolution (between 0.3 and 1.1 km) will have a strong impact on the estimates of the diagnostics. The level of the ozone minimum is often not well defined in zonal mean data because the mid-tropospheric vertical gradients in ozone are small. Thus we refrain from showing these diagnostics for zonal mean output.

Trends calculated using WACCM and CMAM 3-D monthly mean fields on model pressure levels are used to estimate the diagnostics at each point. We compare the zonal mean of the point-by-point trends on model levels to trends estimated using zonal mean temperature and ozone interpolated to a standard set of levels for each diagnostic For the diagnostics in Sect. 4, the individual annual tropical means in WACCM have a linear correlation of $\sim$0.96 between diagnostics calculated with 2-D (zonal mean) and 3-D output

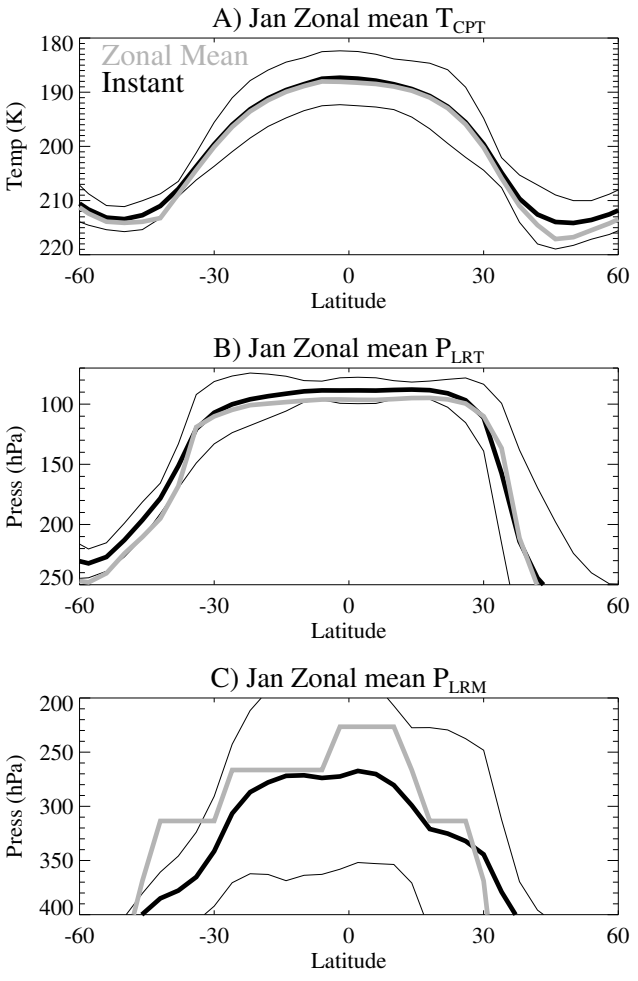

Fig. 1. Comparison between TTL diagnostics calculated using instantaneous WACCM January 3-D output (Black) and zonal mean monthly output (Gray) for Cold Point tropopause temperature (T_{CPT}-top), lapse rate tropopause pressure (P_{LRT}-middle) and lapse rate minimum pressure (P_{LRM}-bottom). Two standard deviation (2σ) zonal range for 3-D output is shown by thin solid lines.

fields (temperature and ozone). The trends in WACCM and CMAM calculated in different ways differ by only a few percent, and are not statistically different. We expect the trend consistency to be valid for models which interpolated their output using all model levels when data was put into the archive, as discussed by Son et al. (2008) for a subset of these models. The GEOSCCM model has undergone interpolation for tracer fields after saving only a limited number of levels, and MRI interpolated twice, which may effect trends. GEOSCCM and MRI are not reported in the multi-model ensemble trend numbers, but are shown on the plots.

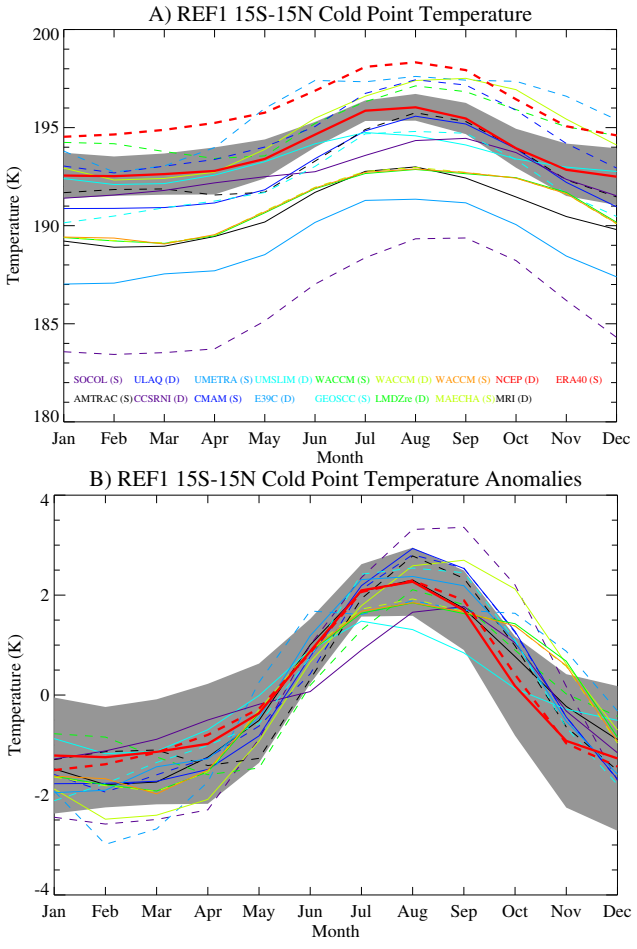

Fig. 2. Annual Cycle of Tropical (15 S–15 N) Zonal mean Cold Point Temperature (T_{CPT}) from REF1 (1979–2001) scenarios of CCMVal Models. **(A)** Temperature. **(B)** Temperature anomalies (annual mean removed). Thick Red lines are NCEP/NCAR (dotted) and ERA40 (solid) Reanalysis. Gray shading is ±2 standard deviations from ERA40. Models are either solid (*S*) or dashed (*D*) lines as indicated in the legend.

3 Multi-model climatology

First we show a few examples of the climatology from the multi-model ensemble from the historical scenarios to verify that CCMs beyond WACCM and CMAM analyzed by GB2007 reproduce the basic structure of the TTL.

Figure 2 illustrates the mean annual cycle of tropical T_{CPT} for 1980–2000. The full field is shown in Fig. 2a and anomalies about the annual mean (highlighting the annual cycle) are shown in Fig. 2b. Models are shown with solid (*S*) or dashed (*D*) lines as indicated in the legend for Fig. 2a. The analysis is nearly the same as that for 100 hPa Temperatures shown in Fig. 7 of Eyring et al. (2006). The amplitude of the annual cycle of T_{CPT} (4 K) is similar to the annual cycle amplitude of 100 hPa temperatures (4 K) in ERA40, and the seasonality is the same.

All models have the same annual cycle of T_{CPT} (Fig. 2b), to the extent that the peak-to-peak amplitude is 3–5 K with a minimum in December–February and a maximum in August–September. This is also true for the Lapse Rate Tropopause Temperature (not shown). Tropical mean T_{CPT} is lowest in December–March, and highest in August–September. There are some models in which the annual cycle is shifted by 1–2 months relative to the reanalysis (red lines in Fig. 2). The amplitude of annual cycle is 4–5 K in most models (Fig. 2b), but the absolute value varies by 10 K (Fig. 2a). Note that the analysis systems (ERA40 and NCEP) are also different, with NCEP warmer. The differences in analysis systems is due to differences in use of satellite temperature data and radiosonde data (Pawson and Fiorino, 1999). The reasons for the differences in simulated T_{CPT} are likely to be complex, having to do both with model formulation and the use of monthly mean output. T_{CPT} is analyzed from monthly mean output on standard levels and may not be relevant for water vapor, since 3-D transport plays a role (see Sect. 5). The difference in T_{CPT} between CCMs is partially due to slight differences in the pressure of the minimum temperature, which varies similarly to the P_{LRT} (see Fig. 5 below). GB2007 have shown for WACCM and CMAM overall agreement of T_{CPT} and P_{LRT} with radiosonde and Global Positioning System (GPS) radio occultation observations in both the mean and standard deviation.

Differences between 3-D WACCM or 3-D CMAM (calculated on model levels using 3-D monthly means) and 2-D WACCM or 2-D CMAM (calculated on standard CCMVal levels using zonal means as input) indicate about 1–2 K temperature differences between 2-D and 3-D, (Fig. 1a). Thus for CMAM and WACCM the effect of averaging and interpolation to standard vertical levels is small. However, the difference makes it somewhat difficult to relate the differences in T_{CPT} to differences in water vapor (shown by Eyring et al. (2006) for these runs). The reanalysis systems have warmer T_{CPT} than most models, which may be a bias in the analysis (Pawson and Fiorino, 1999), or due to coarse vertical resolution (Birner et al., 2006). The inter-annual variability, shown as a 2σ confidence interval for the reanalysis in Fig. 2a, is about 2 K.

Figure 3a illustrates the annual zonal mean P_{LRT}. The lapse rate tropopause pressure is a better metric than the cold point tropopause pressure for trends, because in many cases the cold point is always the same level (it is not interpolated). T_{CPT} at a constant level occurs when variability is less than the model vertical grid spacing. However, we note that T_{ZLR} (the cold point interpolated in pressure) is close to T_{CPT}, and we have also examined P_{ZLR}, which is within 10 hPa of P_{LRT}, and is highly correlated in space and time. The seasonal cycle is not shown, but the P_{LRT} is lowest (highest altitude) in February–April (flat in winter), and maximum, (lowest altitude) in July–October. There is more variation seasonally between models, but models are generally clustered with an annual tropical mean of between

92–102 hPa (P_{LRT} is interpolated) and an annual cycle amplitude of about 10 hPa. There is more variation between models poleward of 30° latitude.

The P_{LRM} is illustrated in Fig. 3b. P_{LRM} is generally around 250 hPa in the deep tropics (15 S–15 N latitude), with 2 models near 200 hPa, and scatter below this. There is little annual cycle in most models (not shown). P_{LRM} is well defined in convective regions (see GB2007 for more details) within ∼20° of the equator. It is not well defined outside of the deep tropics and is not a useful diagnostic there.

4 Long term trends

As noted in Sect. 2.3 we have analyzed trends from WACCM and CMAM with both 3-D and zonal monthly mean data, and found no significant differences in P_{LRT}, T_{CPT} or P_{LRM}. For WACCM the correlation between 3-D and 2-D annual means is ∼0.96. So for estimating trends, we use the zonal monthly mean data available from all the models. We start with historical trends (REF1: 1960–2001) in Sect. 4.1 and then discuss scenarios for the future in Sect. 4.2. Table 3 summarizes multi-model and observed trends for various quantities, with statistical significance (indicated by an asterisk in the table) based on the 2σ (95%) confidence intervals from a bootstrap fit of the multi-model ensemble mean time-series. For the last three columns, not all models provide output over the entire time period (see for example, Fig. 4). Eleven models are included in statistics for REF1 and nine for REF2. E39C and UMETRAC REF2 runs were not available, and the GEOSCCM and MRI values were not included due to double interpolation. ULAQ is not included for analysis of P_{LRM} due to resolution.

4.1 Historical trends

Little change is evident from 1960–2005 in simulated T_{CPT} (Fig. 4). It is hard to find any trends which are significantly different from zero in the simulations (Table 3). Some models appear to cool, some to warm, but these do not appear to be significant trends. However, many models and the reanalysis systems do indicate cooling from 1991–2004. The result is consistent with Fig. 2 of Eyring et al. (2007) that shows the vertical structure of tropical temperature trends. There is a significant negative trend in T_{CPT} estimated from radiosonde analyses. NCEP reproduces the trend, but ERA40 does not. However, the NCEP trend may be spurious (Randel et al. (2006), and references therein) resulting from changes in input data over time. Thus there is also significant uncertainty in T_{CPT} trends in the reanalysis data. Radiosonde trends are considered more robust (Seidel and Randel, 2006).

The Lapse Rate Tropopause Pressure (P_{LRT}) does appear to decrease in the simulations (Fig. 5) and in the reanalyzes, indicating a lower pressure (higher altitude) to the tropical tropopause of −1 to −1.5 hPa/decade (Table 3). However,

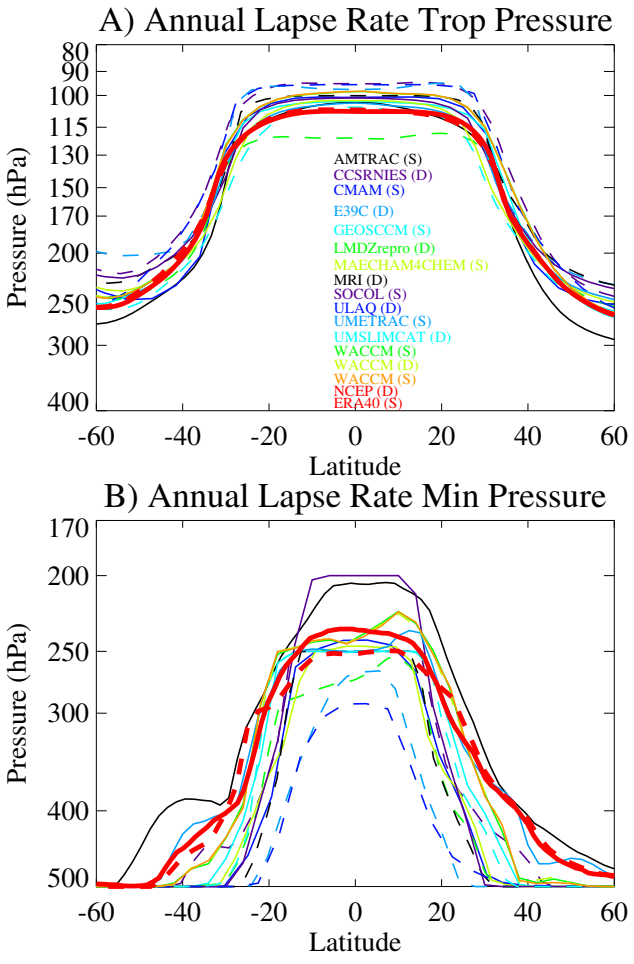

Fig. 3. Zonal mean **(A)** Lapse Rate Tropopause Pressure (P_{LRT}) and **(B)** Lapse Rate Minimum Pressure (P_{LRM}) from CCM-Val models (REF1 scenarios, 1979–2001). Thick Red lines are NCEP/NCAR (dashed) and ERA40 (solid) Reanalyses. Models are either solid (*S*) or dashed (*D*) lines as indicated in the legend in (A). Vertical levels used are noted by tick marks on the vertical axis.

there is no trend in radiosonde analyses of P_{LRT} from 1979–2001. Other analyses with the Parallel Climate Model (Santer et al., 2003), a subset of these models (Son et al., 2008) and observations (Seidel et al., 2001; Gettelman and Forster, 2002) do show decreases in P_{LRT}. Simulated P_{LRT} trends are of the same sign and magnitude as P_{ZLR} trends. In general the trend is consistent across models in Fig. 5. Inter-annual variability in any model is generally less than in the reanalyses or radiosondes. As noted, T_{CPT} is correlated with CPT pressure. The correlation can be seen in the P_{LRT} as well in Fig. 5: models with lower pressure P_{LRT} have lower T_{CPT} (Fig. 4).

These tropopause changes represent changes in the "top" of the TTL. The "bottom" of the TTL is represented by the Lapse Rate Minimum pressure (P_{LRM}), which is related to

Table 3. Trends (per decade "*d*") in Key TTL quantities from analysis systems (NCEP/NCAR and ERA40) and model simulations. Trends significantly different from zero (based on 2σ confidence intervals, or 95% level) indicated with an asterix. 13 models are included in statistics for REF1 and 10 for REF2.

Diagnostic	Units	NCEP/NCAR 1979–2001	ERA40 1979–2001	RAOBS 1979–2001	Sim REF1 1979–2001	Sim REF1 1960–2004	Sim REF2 1980–2100	Sim REF2 1980–2050
T_{CPT}	K/d	−0.94*	0.54*	−0.68*	−0.03	−0.04	0.09*	0.09*
T_{ZLR}	K/d	−1.1*	0.53*		−0.03	−0.03	0.10*	0.10*
P_{ZLR}	hPa/d	−0.28	−0.86*		−0.58*	−0.72*	−0.53*	−0.60*
P_{LRT}	hPa/d	−1.0*	−1.3*	0.0	−0.75*	−0.66*	−0.60*	−0.64*
P_{LRM}	hPa/d	−2.8*	−15*	−0.36	−2.6*	−0.25	−2.6*	−2.3*

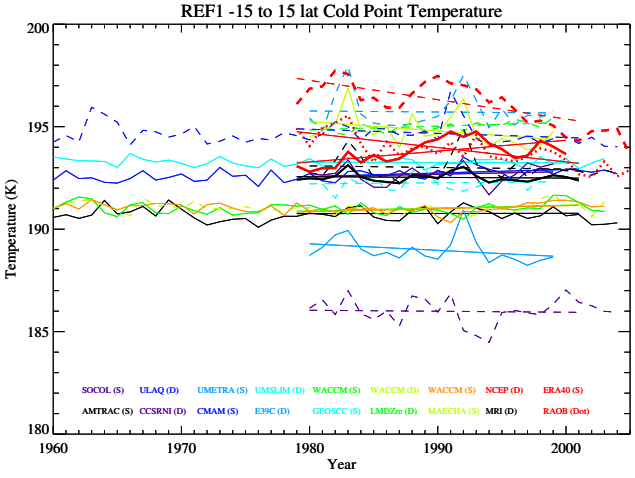

Fig. 4. Tropical mean Cold Point Tropopause Temperature (T_{CPT}) from various models for Historical (REF1) runs. Thin lines are linear trends. Models are either solid (*S*) or dashed (*D*) lines as indicated in the legend. Thick red lines are NCEP/NCAR (dashed), ERA40 (solid) Reanalyses and thick red dotted line is radiosonde annual anomalies as described in the text. Thick black line is the multi-model mean anomalies added to the ERA40 inter-annual mean as described in the text.

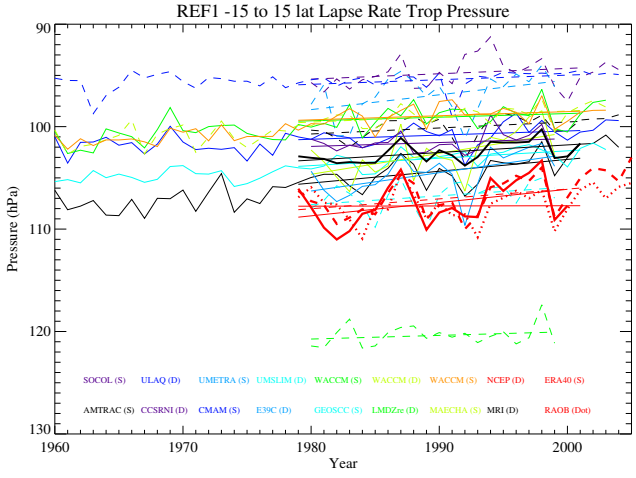

Fig. 5. Tropical mean Lapse Rate Tropopause Pressure (P_{LRT}) from various models for Historical (REF1) runs. Thin lines are linear trends. Models are either solid (*S*) or dashed (*D*) lines as indicated in the legend. Thick red lines are NCEP/NCAR (dashed), ERA40 (solid) Reanalyses and thick red dotted line is radiosonde annual anomalies as described in the text. Thick black line is the multi-model mean anomalies added to the ERA40 inter-annual mean as described in the text.

the main convective outflow, and thus a measure of where convection impacts the thermodynamic profile in the TTL. Trends in P_{LRM} are shown in Fig. 6. Large variability and a higher P_{LRM} in ULAQ is likely due to coarse vertical (2500 m) and horizontal resolution ($10° \times 22.5°$).

The multi-model trend in P_{LRM} for the 1979–2001 is significant, with a P_{LRM} decrease of −2.6 hPa/decade. ERA40 shows a large (−15 hPa/decade) decrease in P_{LRM}, mostly from 1990–2001. However, radiosondes show no significant trend in P_{LRM}. The reason for the discrepancy in the analysis systems and radiosondes is not known, but may be due to limited radiosonde sampling. The LRM level can vary with unconstrained parts of model convective parameterizations in both CCMs and reanalyses. Thus the diagnostic may not be quantitatively robust. However, the P_{LRT} in Fig. 5 is much more tightly constrained, with both analysis systems highly correlated, and many of the models also having correlated inter-annual variability, most likely forced by Sea Surface Temperature patterns (ENSO).

To better understand the above trends, we have analyzed T_{CPT} (Fig. 7a), P_{LRT} (Fig. 7b) and P_{LRM} (Fig. 7c) trends at each grid point in the REF1 WACCM simulations using 3-D monthly mean output. The trends are indicated in Fig. 7, along with trends in cloud top pressure by location (Fig. 7d). Shaded trends more than one contour interval from zero in Fig. 7 are almost always significant at the 95% (2σ) level. The figure represents an average of trends from all 3 WACCM REF1 realizations, which all have similar patterns. WACCM has moderate correlations with reanalysis

P_{LRT} (Fig. 5), but with less inter-annual variability. WACCM has less variability because it does not include the aerosol effects of significant volcanic eruptions (such as Mt. Pinatubo in 1991 or El Chichon in 1983).

In Fig. 7a simulated T_{CPT} decreases throughout the tropics in WACCM and increases in the subtropics. WACCM simulated T_{CPT} changes are largest centered over the Western Pacific, but simulated T_{CPT} actually increases over Tropical Africa. The simulated zonal mean trend is not significant. These changes can be partially explained with the pattern of changes in simulated cloud top pressure (Fig. 7d) in WACCM, with decreasing pressure (higher clouds) in the Western Pacific and increasing pressure (lower clouds) in the Eastern Pacific. The clouds appear to shift towards the equator from the South Pacific Convergence Zone (SPCZ), with increasing cloud pressure north of Australia in the WACCM simulations. Figure 7b shows that the simulated P_{LRT} has decreased almost everywhere in the tropics and sub-tropics, with largest changes in the Eastern Pacific. Simulated P_{LRM} (Fig. 7c) does not have a coherent trend in WACCM, consistent with Fig. 6.

There are very large differences in mean 300 hPa ozone in the tropical troposphere in the models (Fig. 8b). 300 hPa is a level near the ozone minimum. The differences are expected since tropospheric ozone boundary conditions were not specified, and the models have different representations of tropospheric chemistry. The spread of ozone at 300 hPa is 10–80 ppbv with most models clustered around the observed value of 30 ppbv (from SHADOZ Ozonezondes). CMAM ozone (the lowest) is low due to a lack of tropospheric ozone sources or chemistry which may impact T_{CPT}.

Even at 100 hPa near the tropopause there are variations in ozone between 75–300 ppbv (Fig. 8a). The values get larger than the ∼120 ppbv observed from SHADOZ. Most models have a low bias relative to SHADOZ. Several models are not clustered with the others in Fig. 8a, including LMDZ, MAECHAM, MRI, SOCOL and ULAQ. For MAECHAM this is related to low ascent rates in the lower stratosphere (Steil et al., 2003). There is also a positive correlation (linear correlation coefficient ∼0.6) between average Cold Point Temperature and average ozone in models around the tropopause (150–70 hPa). Models with higher ozone have higher tropopause temperatures in Fig. 2, consistent with an important role for ozone in the radiative heating of the TTL. It may also result from differences in dynamical processes (slower uplift would imply both higher temperatures and higher ozone). We discuss this further in Sect. 5.

4.2 Future scenarios

We now examine the evolution of the TTL for the future scenario (REF2). As discussed in Eyring et al. (2007), the future scenario uses near common forcing for all models. Models were run from 1960 or 1980 to 2050 or 2100. Surface concentrations of greenhouse gases (CO_2, CH_4, N_2O) are specified from the Intergovernmental Panel on Climate Change (IPCC) Special Report on Emissions Scenarios (SRES) GHG scenario A1b (medium) (IPCC, 2000). Surface halogens (chlorofluorocarbons (CFCs), hydro-chlorofluorocarbons (HCFCs), and halons) are prescribed according to the A1b scenario of World Meteorological Organization (2003). Sea surface temperatures (SSTs) and sea ice distributions are derived from IPCC 4th Assessment Report simulations with the coupled ocean-atmosphere models upon which the CCMs are based. Otherwise, SSTs and sea ice distributions are from a simulation with the UK Met Office Hadley Centre coupled ocean-atmosphere model HadGEM1 (Johns et al., 2006). See Eyring et al. (2007) for details. Trends in Table 3 are calculated from available data for each model from 1980 to 2050, since only 3 CCMs (AMTRAC, CMAM, GEOSCCM) are run to 2100. Future trends are broadly linear, and trends for those models run to 2100 are not significantly different if the period 1980–2100 is used (the last two columns are nearly identical. Trends are slightly larger for 2000–2050, likely due to additional forcing from ozone recovery.

Figure 9 illustrates changes in T_{CPT}, similar to Fig. 4 but for the future (REF2) scenario. Models generally project cold point or lapse rate tropopause temperatures to increase slightly. The multi-model rate of temperature increase is only 0.09 K/decade (Table 3), but is significant. For AMTRAC, the increase is almost 0.3 K/decade in the early part of the 21st century. The increase may be related to the low ozone at the tropopause (Son et al., 2008). The analysis is consistent

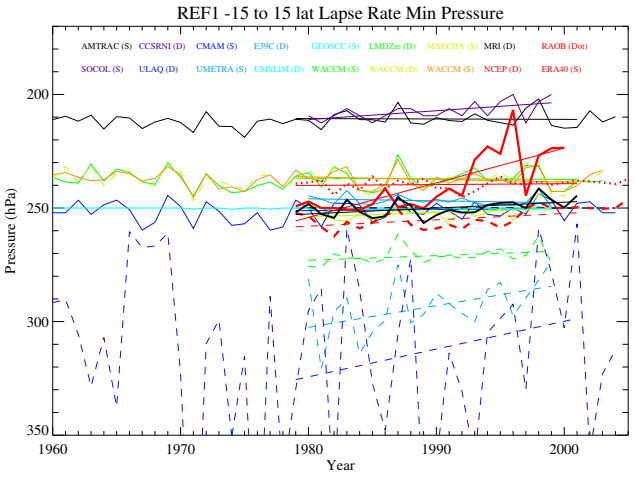

Fig. 6. Tropical mean Lapse Rate Minimum Pressure (P_{LRM}) from various models for Historical (REF1) runs. Thin lines are linear trends. Models are either solid (*S*) or dashed (*D*) lines as indicated in the legend. Thick red lines are NCEP/NCAR (dashed), ERA40 (solid) Reanalyses and thick red dotted line is radiosonde annual anomalies as described in the text. Thick black line is the multi-model mean anomalies added to the ERA40 inter-annual mean as described in the text.

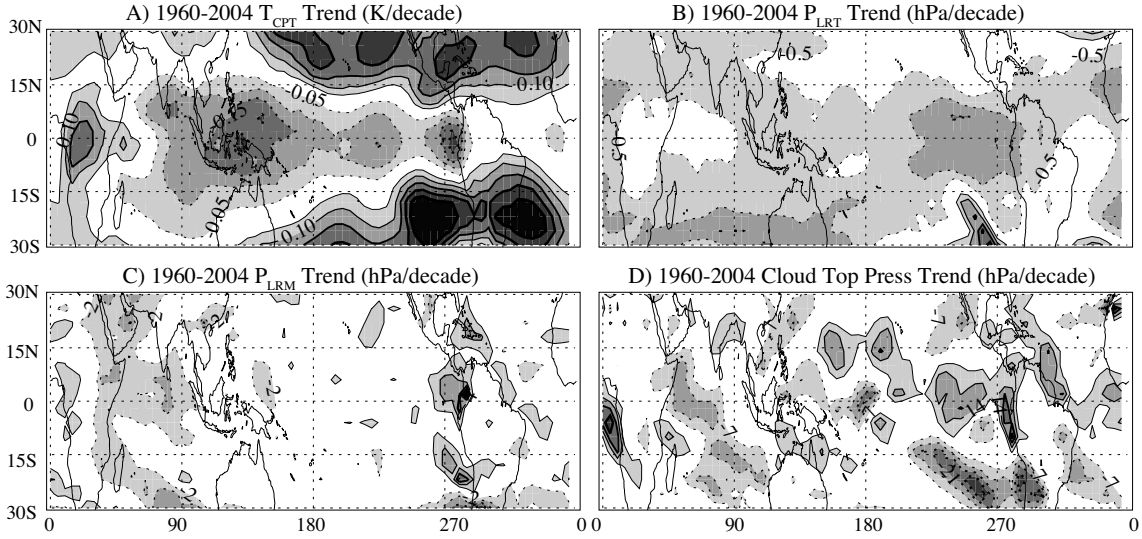

Fig. 7. Map of trends from historical (REF1) WACCM simulations. Figure shows average of trends from 3 simulations. **(A)** Cold Point Tropopause Temperature (T_{CPT}) trends, contour interval 0.05 K/decade. **(B)** Lapse Rate Tropopause pressure (P_{LRT}) trends, contour interval 0.5 hPa/decade **(C)** Lapse Rate Minimum Pressure (P_{LRM}) trends, contour interval 2 hPa/decade. **(D)** Cloud Top Pressure trends, contour interval 7 hPa/decade. Dashed lines are negative trends, no zero line.

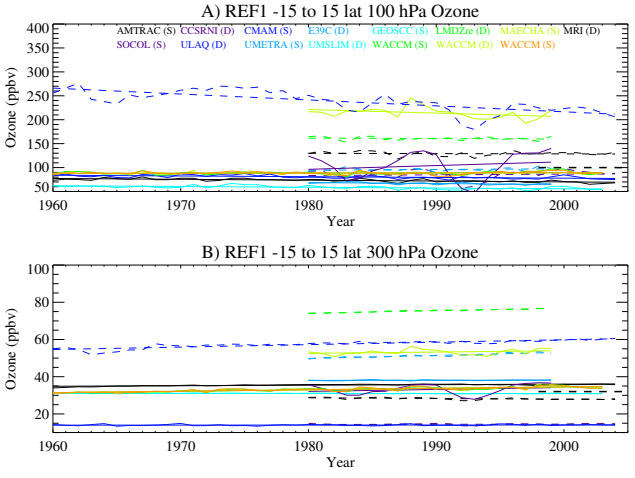

Fig. 8. Tropical mean Ozone from various models at **(A)** 100 hPa and **(B)** 300 hPa. Thin lines are linear trends. Thick black dashed lines are the SHADOZ observed mean from 1998–2005 at these levels. Models are either solid (*S*) or dashed (*D*) lines as indicated in the legend.

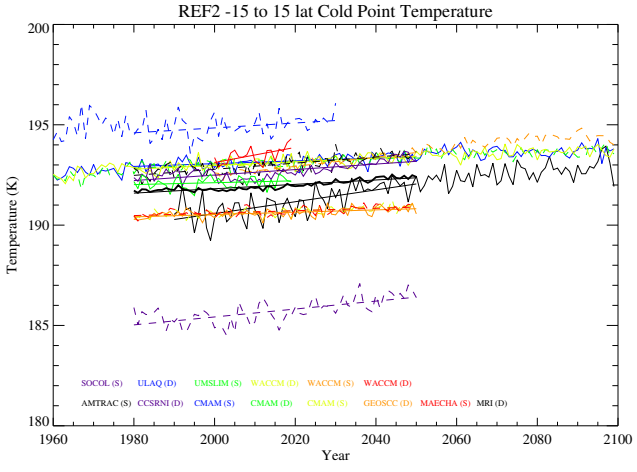

Fig. 9. Tropical mean Cold Point Tropopause Temperature (T_{CPT}) from various models showing expected future scenarios (REF2). Thin lines are linear trends. Models are either solid (*S*) or dashed (*D*) lines as indicated in the legend. Thick black line is the multi-model mean anomalies added to the multi-model inter-annual mean.

with Fig. 2 of Eyring et al. (2007) that shows the vertical structure of tropical temperature trends.

In addition to the small temperature increase, simulated P_{LRT} decreases as well (altitude increase), seen in Fig. 10. The rate of decrease of the multi-model ensemble is −0.64 hPa/decade, less than observed during the historical record in REF1 scenarios or observed in the reanalyses (Table 3). However, there is consistency among most of the model trends. All models except one have the same sign of the trend, though with some spread in magnitude (Fig. 10). The ∼15 hPa spread in pressure is likely due to different model formulations and vertical resolution.

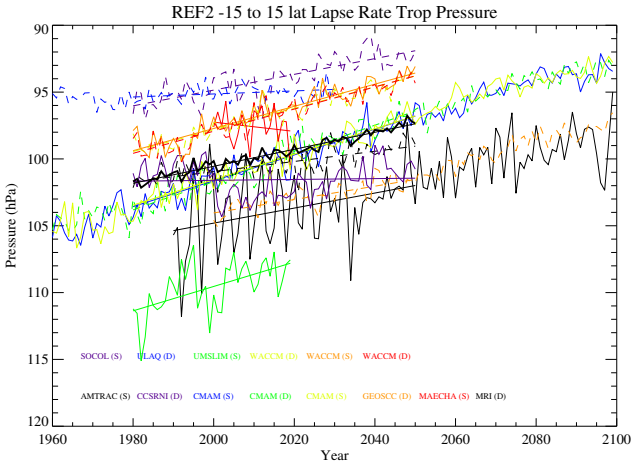

Fig. 10. Tropical mean Lapse Rate Tropopause Pressure (P_{LRT}) from various models showing expected future scenarios (REF2). Thin lines are linear trends. Models are either solid (S) or dashed (D) lines as indicated in the legend. Thick black line is the multi-model mean anomalies added to the multi-model inter-annual mean.

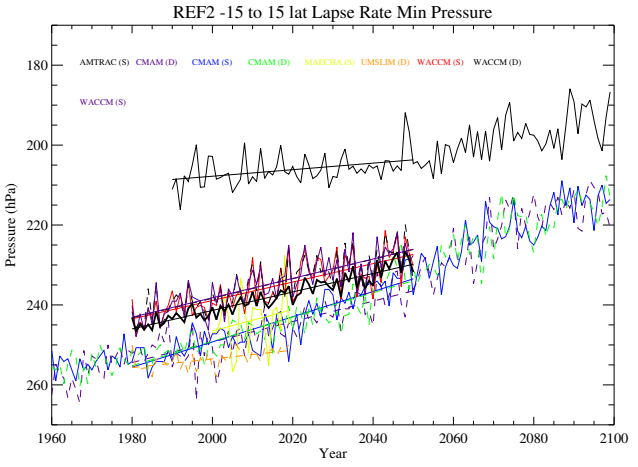

Fig. 11. Tropical mean Lapse Rate Minimum Pressure (P_{LRM}) from various models showing expected future scenarios (REF2). Thin lines are linear trends. Models are either solid (S) or dashed (D) lines as indicated in the legend. Note that ULAQ is off scale. Thick black line is the multi-model mean anomalies added to the multi-model inter-annual mean.

Figure 11 indicates that the P_{LRM} decreases significantly in some simulations (CMAM, WACCM, AMTRAC, MAECHAM), and does not change in others (SOCOL). In some simulations (MRI), the P_{LRM} is not well defined, and its pressure is indeterminate. In other simulations (CMAM) there are apparent differences in trend before and after 2000. Since the P_{LRM} represents the impact of convection on thermodynamics, differences are likely due to different convective parameterizations in the simulations. For the multi-model ensemble, the change is -2.3 hPa/decade, and is significant. Changes in the P_{LRM} indicate changes in the outflow of convection in the upper troposphere. The changes in P_{LRM} and P_{LRT} together imply a thinner TTL (in mass).

Figure 12 illustrates the map of trends for WACCM from the REF2 runs from 1975–2050. As with Fig. 7, the map is an average of 3 runs with similar patterns. WACCM simulated trends in T_{CPT} are smaller than some models (Fig. 9). WACCM simulated P_{LRT} trends are of similar magnitude to other models (Fig. 10). Figure 12a indicates that simulated T_{CPT} increases in most regions of the tropics. Simulated T_{CPT} trends are largest (0.2 K/decade) over 0–120 E (Africa–Indonesia). Simulated T_{CPT} does not change over the subtropical Pacific. In addition, clouds go up to higher altitudes, trends up to -14 hPa/decade, over the Central Pacific (Fig. 12d) extending into the Western Pacific. The changes are consistent with 21st century rainfall anomalies in the underlying GCM for WACCM (Meehl et al., 2006). These changes are not necessarily consistent in multi-model projections of changes in precipitation (Solomon et al., 2007). The simulated T_{CPT} trend pattern is consistent with decreasing temperatures from enhanced Central Pacific heating. The pattern is the same as that observed for the historical record (Fig. 7, see Section 4.1), superimposed on an overall warming.

Simulated P_{LRT} appears to decrease everywhere in the tropics (Fig. 12b). There is not much structure to the decrease, though it is larger over the Central Pacific where clouds are going higher in WACCM (Fig. 12d). Simulated P_{LRM} (Fig. 12c) also goes up in most regions of the tropics. The pattern does not have much structure. There are larger changes near the coast of South America. Simulated changes do not appear to be associated with changes in cloud pressure (Fig. 12d). It may be that another variable would be better suited to looking at coupling between cloud detrainment and the P_{LRM}, but only limited diagnostics are available. These diagnostics do not indicate as direct a connection between clouds and P_{LRM} changes as seen in REF1 runs (Fig. 7).

The Zero Lapse Rate (ZLR) pressure (P_{ZLR}) and temperature (T_{ZLR}) are another way to examine the thermal structure around the tropopause. The ZLR is defined identically to the Lapse Rate Tropopause, but for a lapse rate of 0 K/km not -2 K/km. It also defines the cold point, but can be interpolated from coarse temperature profiles. The T_{ZLR} and P_{ZLR} trends are indicated in Table 3, and are basically identical to T_{CPT} and P_{LRT} trends. T_{ZLR} and P_{ZLR} trends from the REF1 scenarios and reanalyses (not shown) are of the same sign (Fig. 4 and Fig. 5). The sign of the trends for T_{ZLR} and P_{ZLR} is also the same as T_{CPT} and P_{LRT} trends for the REF2 scenarios (Figs. 9 and 10). The ZLR trends serve as a consistency check on the derived tropopause trends.

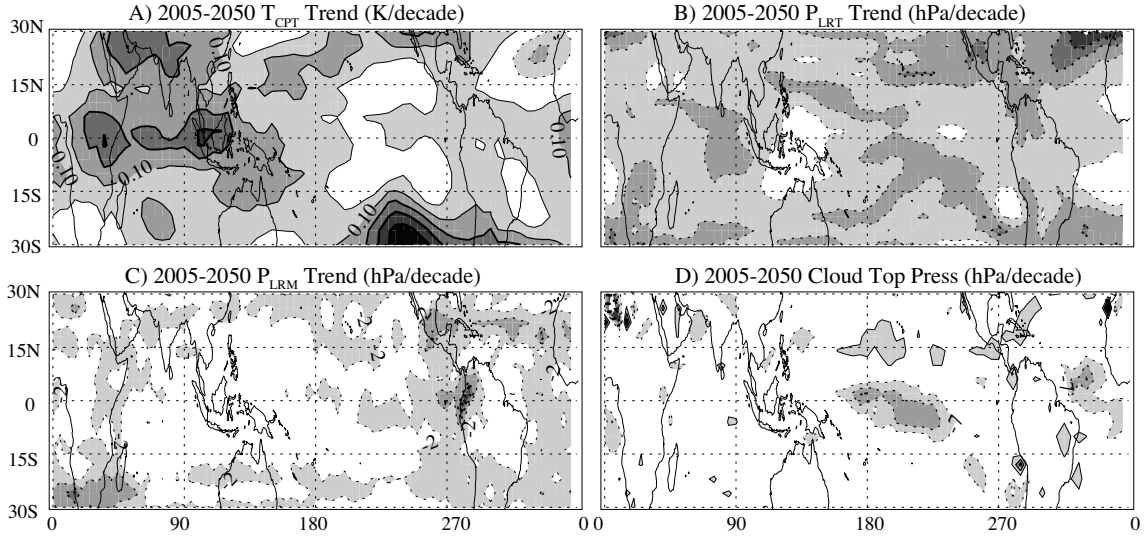

Fig. 12. Map of trends from future (REF2) WACCM simulations. Figure shows average of trends from 3 simulations. **(A)** Cold Point Tropopause Temperature (T_{CPT}) trends, contour interval 0.05 K/decade. **(B)** Lapse Rate Tropopause pressure (P_{LRT}) trends, contour interval 0.5 hPa/decade **(C)** Lapse Rate Minimum Pressure (P_{LRM}) trends, contour interval 2 hPa/decade. **(D)** Cloud Top Pressure trends, contour interval 7 hPa/decade. Dashed lines are negative trends, no zero line.

5 Discussion

Finally we address three derived questions that result from these simulations. First, we look at why Cold Point Temperatures increase but the tropopause rises (decreases in pressure) and causes of these changes. Second, we try to use the spread of model ozone values to ask if ozone effects the TTL structure. Third, we look at the implications of tropopause temperature changes on stratospheric water vapor.

5.1 Tropopause changes

It is useful to consider the geometric picture of tropopause trends for an analysis of changes in tropopause temperature given changes in tropopause height (or pressure) and changes in tropospheric and stratospheric temperature, respectively. Assume that the temperature profile is piecewise linear and continuous in height with distinct tropospheric and stratospheric temperature gradients Γ_t and Γ_s, respectively: $T{=}\Gamma_t z{+}T_{\mathrm{sfc}}$ for $z{\leq}z_{\mathrm{TP}}$ and $T{=}\Gamma_s z{+}T_{0\mathrm{s}}$ for $z{\geq}z_{\mathrm{TP}}$. Here, z_{TP} refers to tropopause height, T_{sfc} refers to surface temperature and its changes represent tropospheric temperature trends, and $T_{0\mathrm{s}}$ is the temperature at which the stratospheric profile would intersect the ground and its changes represent stratospheric temperature trends. It is straight forward to combine both tropospheric and stratospheric temperature profiles to yield tropopause temperature:

$$T_{\mathrm{TP}}{=}\frac{\Gamma_t{+}\Gamma_s}{2}z_{\mathrm{TP}}{+}\frac{T_{\mathrm{sfc}}{+}T_{0\mathrm{s}}}{2}\,.$$

Potential trends in tropical tropopause temperature thus result from the combined trends in tropospheric and stratospheric temperatures. Since these are of opposite sign, and the sign changes in the vicinity of the tropopause, it is not clear from simple analytical arguments whether tropopause temperature will increase or decrease. It depends on the balance of the terms in the equation above.

Changes to the TTL given greenhouse gas forcing imply that the tropical tropopause pressure should decrease due to stratospheric cooling or due to tropospheric warming (see below). However, it is not clear what should happen to tropopause temperature. If the troposphere warms, the upper troposphere may warm by a larger amount than the surface (Santer et al., 2005). Assuming no change to stratospheric temperatures, the change would push the tropopause to higher altitudes (lower pressures) and higher temperatures. If the stratosphere cools and the troposphere stays constant, the change would push the tropopause to higher altitudes (lower pressures) and lower temperatures.

In reality, radiative forcing by anthropogenic greenhouse gases both warms the troposphere (increasing T_{sfc}) and cools the stratosphere (Solomon et al., 2007). Stratospheric cooling will change $T_{0\mathrm{s}}$, depending on the structure and magnitude of the temperature change. The changes are illustrated in the vertical profile of temperature trends from these simulations, Fig. 2 of Eyring et al. (2007). The change from warming to cooling is right around the tropopause.

Thus we expect tropopause rises, but what will happen to its temperature? Figure 13 illustrates 1980 (solid) and 2050 (dashed) profiles from WACCM (orange-red) and CMAM

(purple) realizations. Here it is clear that the troposphere is warming, and the stratosphere is cooling, but the result is a slight warming of the tropopause temperature. The response seems consistent across all model simulations (Fig. 9). As noted by Son et al. (2008) this is dependent upon ozone recovery, and may be different for those models without interactive ozone chemistry. We further note that for WACCM and CMAM, as well as most other models, Γ_s is increasing in magnitude (more negative) in the stratosphere due to greenhouse gas induced cooling. Γ_t is increasing in the upper troposphere at 250 hPa (due to tropospheric warming). The change in sign of the trends is at ≈200 hPa, 100 hPa below the tropopause. The location of the change may imply that over the long term, surface processes (convective equilibrium) have less of a direct influence on the trends at 150 hPa and lower pressures.

Another way of looking at causes of changes in tropopause height is to do a simple multiple linear regression of TTL diagnostics on stratospheric temperature and surface temperature. We performed a simple multiple linear regression on annual anomalies of tropical (15 S–15 N) mean T_{CPT}, P_{LRT} and P_{LRM}, against annual tropical mean anomalies of stratospheric (50 hPa) temperature and surface (1000 hPa) temperature. We have included ozone concentrations at various levels and report those configurations that maximize the fit. The regressions are judged by the percent of variance explained, and individual terms evaluated by the effect on the TTL diagnostic: °C (T_{CPT}), hPa (P_{LRT} and P_{LRM}) per standard deviation (σ) of the predictor (T_{1000}, T_{50}, O_3). We have performed regression on each model time-series included in the multi-model mean for REF2, with available ozone and temperature data: 5 models with 9 realizations: AMTRAC, CMAM (3 realizations), MAECHAM, UMSLIMCAT and WACCM (3 realizations). Regression results are consistent across CCMs. Below we report means across 9 realizations.

Approximately 77% of the interannual variance in tropical averaged T_{CPT} can be explained by multiple regression with just 1000 hPa and 50 hPa temperature, and 100hPa Ozone. Where higher T_{1000}, T_{50} or O_3 corresponds to a warmer tropopause. Surface temperature is the most important (0.7°C/σT_{1000}) followed by 100 hPa Ozone (0.3°C/σO_3) and 50 hPa temperature (0.2°C/σT_{50}). For P_{LRT} a regression with surface temperature, 50hPa temperature and 100 hPa ozone explains ∼91% of the variance. Higher ozone at 100 hPa implies higher P_{LRT} (0.9 hPa/σO_3) and warmer surface temperatures correlate with lower P_{LRT} (higher tropopause by −0.7 hPa/σT_{1000}). Colder stratospheric temperatures correlate with higher P_{LRT} (0.4 hPa/σT_{50}). For P_{LRM} the surface temperatures dominate (81% of interannual variance explained), and an increasing surface temperature causes a decrease in P_{LRM} of −9 hPa/σT_{1000}. The ozone effect is smaller, and largest for lower tropospheric ozone (700 hPa: 2.7 hPa/σO_3), and the effect of the stratospheric temperatures is small (1.5 hPa/σT_{50}).

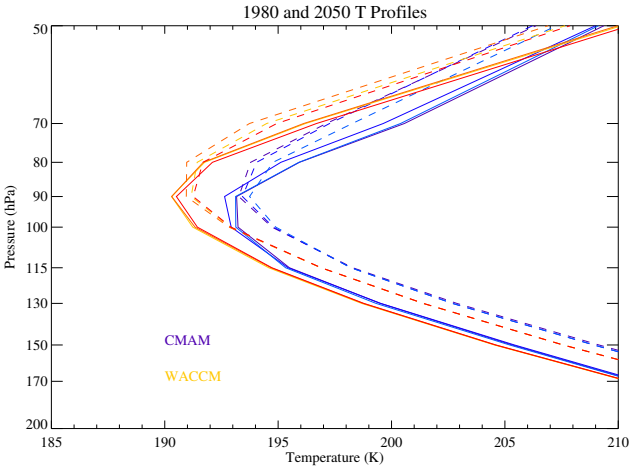

Fig. 13. Tropical temperature profiles from WACCM and CMAM models for future (REF2) scenarios. Solid lines: 1980 average. Dashed lines: 2050 average for each of 3 realizations.

5.2 Ozone impacts on tropopause

Given the wide variation and differences in ozone (Fig. 8), this is a natural experiment to see if ozone matters for the structure of the TTL, as discussed by Thuburn and Craig (2002). It does appear that tropopause level (100 hPa) ozone is correlated with temperature: those models with colder T_{CPT} (Fig. 4) do appear to have less ozone at 100 hPa (Fig. 8), the correlation between average tropical ozone and T_{CPT} across 13 models is 0.6. Multiple linear regression discussed above supports the basic correlation, indicating that near tropopause ozone affects both T_{CPT} and P_{LRT}.

It is not clear whether ozone differences are due to transport or chemistry. For some models (i.e. CMAM) low ozone is due to missing chemical processes (i.e. lightning NOx production for CMAM). For other models, slow ascent may allow ozone to increase photochemically (MAECHAM). A positive temperature – ozone correlation might also result from faster (slower) uplift which cools (warms) temperature and decreases (increases) ozone. In addition, models with a colder tropopause have a higher tropopause, but higher (altitudes) should have more ozone and more heating, indicating that ozone changes may not be the dominant contributor to observed variability.

5.3 Stratospheric water vapor

Tropical tropopause temperatures control stratospheric water vapor (Holton and Gettelman, 2001; Randel et al., 2006). Analysis indicates that the variation in T_{CPT} among the models does strongly affect stratospheric water vapor. Figure 14 shows a scatter-plot of the mean annual saturation vapor mixing ratio (Q_{sat}) at the T_{CPT} for all the models, plotted as a function of mean annual 90 hPa water vapor. Also included

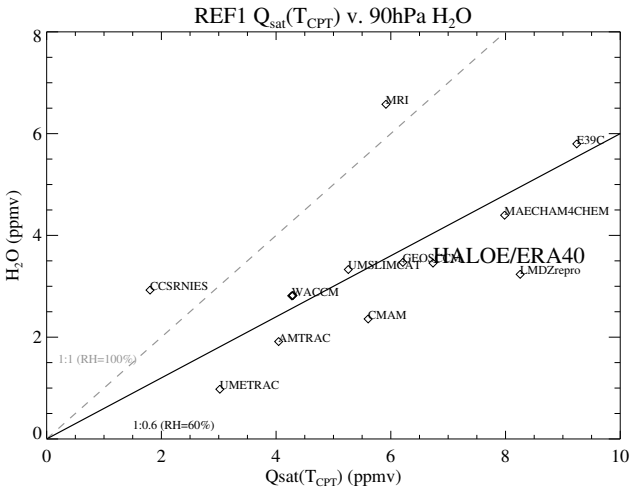

Fig. 14. Scatter-plot of Saturation Vapor Mixing Ratio of the Cold Point Tropopause Temperature, $Q_{\rm sat}$ ($T_{\rm CPT}$) and the 90hPa tropical water vapor mixing ratio fore each historical (REF1) run, as well as using ERA40 temperatures and HALOE 100 hPa water vapor (ERA40/HALOE). Gray dashed line is 1:1 line (100% RH), Black solid line is 1:0.6 (60% RH).Value for each point is the diamond at the lower left corner of the model or observation name.

are points representing analysis $T_{\rm CPT}$ from ERA40 and Halogen Occultation Experiment (HALOE) annual mean 100 hPa water vapor (HALOE data was not available at 90 hPa). NCEP is not shown because of the warm bias of NCEP temperatures at the cold point tropopause. The plot indicates that all models and the analysis systems over the historical record fall below a 1:1 line (100% relative humidity at 90 hPa if limited by the $T_{\rm CPT}$), close to a 1:0.6 (60% at 90 hPa), and that there is a correlation between $T_{\rm CPT}$ and tropical 90hPa water vapor, indicating that $T_{\rm CPT}$ limits stratospheric water vapor. The correlation is a tropical mean, so reflects transport processes as well. Three dimensional transport affects H_2O (Gettelman et al., 2002; Fueglistaler and Haynes, 2005), but we do expect a broad correlation with mean temperatures (Randel et al., 2004). Two models (MRI, CCSRNIES) lie above this line, which may indicate differences in transport, such that air has bypassed the tropical tropopause. Having three dimensional model output from all models would enable further analysis.

The projected increase in tropopause temperature would be expected to increase stratospheric water vapor. The magnitude of the warming to 2100 is only $\sim$1.2 K. For a tropopause at 191 K and 90 hPa, warming would change $Q_{\rm sat}$ by 0.9 ppmv (4.3 to 5.2 ppmv), a 20% increase. Eyring et al. (2007) show that the mean 50 hPa tropical (25 S–25 N) water vapor increase in the models is $\sim$25% (0.5–1 ppmv) by 2100. The increase also includes some effect from increasing methane (though the change should not be large at 50 hPa in the tropics).

The increase in water vapor is thus consistent with the $Q_{\rm sat}$ increase implied by average $T_{\rm CPT}$. It is the case even though average $T_{\rm CPT}$ may not be exactly relevant for water vapor as the tropical tropopause temperatures vary in space and time, and water vapor is transported three dimensionally in the TTL.

6 Conclusions

We have analyzed the representation of the Tropical Tropopause Layer in 13 different Coupled Climate Models designed to represent the stratosphere. Results in this work, building upon analysis by GB2007, indicate that the models are able to reproduce the basic structure of the TTL. GB2007 show in detail that two models (WACCM and CMAM) with 200–400 km horizontal and 1.1 km vertical resolution in the TTL can reproduce the TTL climatology and variability. We have shown here that use of 2-D zonal monthly means on standard levels does not affect the climatology or trends calculated from the simulations.

What simulated results do we have confidence in? We ascribe higher confidence to trends in quantities that (a) have consistent historical trends in observations and models and (b) consistent simulated trends across models in the future. We summarize our findings and confidence below.

1. CCMs are generally able to reproduce past trends in tropopause pressure ($P_{\rm LRT}$). Observed inter-annual variability is reproduced in historical simulations. Models and reanalyses indicate decreases in $P_{\rm LRT}$ in the observed record of similar magnitude (trends within 2σ), a result also found in other studies with radiosonde observations. Differences are correlated and consistent, indicating higher confidence in these trends.

   CCMs consistently show continued decreases in $P_{\rm LRT}$ into the future. $P_{\rm LRT}$ trends are consistent across models. Future simulated trends are of lower magnitude than historical trends. The change in magnitude is likely due to (a) difference evolution of forcings in the A1b scenario and (b) ozone loss in the historical period (REF1) and recovery in the 21st century (REF2). Future trends are slightly larger for the 2000–2050 period versus the entire 1980–2100 period. The differences in trends is consistent with the global results of Son et al. (2008) from a subset of these models (AMTRAC, CMAM, GEOSCCM, WACCM).

2. CCMs are not consistently able to reproduce historical trends in tropopause temperature ($T_{\rm CPT}$). Some of the difference is related to the large (10 K) spread in average $T_{\rm CPT}$. CCMs do reproduce amplitude and phase of the annual cycle in $T_{\rm CPT}$. The spread in $T_{\rm CPT}$ appears to be related to (a) the wide spread of ozone at tropopause levels in the simulations and (b) to different altitudes of

the tropopause. Ozone differences are due to both radiation and possibly transport. Differences in T_{CPT} are correlated with differences in simulated stratospheric water vapor.

CCMs show modest and consistent increases in future T_{CPT}. The "raising and warming" of the tropopause is broadly consistent with theory. But since raising implies adiabatic cooling, temperature changes are sensitive to which of these effects dominates. In these simulations, projected tropospheric warming is larger than stratospheric cooling at the tropopause in the 21st century. We place only moderate confidence in future T_{CPT} trends because of difficulties in reproducing historical trends.

3. Over the observed record there are significant changes in the minimum lapse rate level (P_{LRM}). The magnitude of observed and simulated historical trends is uncertain. The lack of quantitative agreement in historical P_{LRM} trends and dependence on convective parameterization yields lower confidence in future trends.

   There are significant and consistent future decreases in simulated P_{LRM}, amounting to a change of -23 hPa over the 21st century, a significant increase in the mean convective outflow level of $\sim$250 m. The change is dependent on a sub-grid scale process (convection) but is likely driven by surface changes (higher temperatures). As a result there is spread to the model trends. Since P_{LRM} decreases faster than P_{LRT}, simulations imply a "thinning" of the TTL in the 21st century of -1.7 hPa/decade.

4. TTL anomalies and trends are highly correlated with anomalies of near surface tropical temperature. Tropopause pressure and temperature are affected by tropopause level ozone. TTL anomalies are affected less by stratospheric temperatures. The surface warming appears to be the dominant signal in the TTL across almost all models. The result is consistent across models, indicating higher confidence in the conclusion.

5. If tropopause height and particularly temperature trends are to be believed, it may have significant impacts on stratospheric water vapor due to higher temperatures, with increases in water vapor in the stratosphere predicted. There is consistency between models and observations of the correlation of T_{CPT} and H_2O (though the absolute value of T_{CPT} varies).

6. TTL and lower stratospheric ozone anomalies substantially influence TTL diagnostics. TTL ozone varies tremendously in the simulations, and also seems to be correlated with the absolute value of tropopause temperature. It is critical that models do a better job of simulating TTL ozone.

Acknowledgements. Co-ordination of this study was supported by the Chemistry-Climate Model Validation Activity (CCMVal) for WCRP's (World Climate Research Programme) SPARC (Stratospheric Processes and their Role in Climate) project. Thanks to all the CCM groups for their comments on this paper specifically, and generally for their hard work in developing and producing model output. We especially thank those model developers who are not co-authors: J. Austin, T. Nagashima, T. G. Shepherd, S. Pawson, R. S. Stolarski, M. A. Giorgetta, E. Manzini, M. Deushi, N. Butchart, M. P. Chipperfield and R. R. Garcia. Thanks to K. Rosenlof for discussions. Thanks to the British Atmospheric Data Center for assistance with the CCMVal Archive. The National Center for Atmospheric Research is sponsored by the US. National Science Foundation. CCSRNIES research was supported by the Global Environmental Research Fund (GERF) of the Ministry of the Environment (MOE) of Japan (A-071). European CCMVal activities were supported by the European Commission Integrated Project SCOUT-O3.

Edited by: P. Haynes

References

Akiyoshi, H., Sugita, T., Kanzawa, H., and Kawamoto, N.: Ozone perturbations in the Arctic summer lower stratosphere as a reflection of NO_x chemistry and planetary scale wave activity, J. Geophys. Res., 109, D03304, doi:10.1029/2003JD003632, 2004.

Austin, J.: A three-dimensional coupled chemistry-climate model simulation of past stratospheric trends, J. Atmos. Sci., 59, 218–232, 2002.

Austin, J. and Butchart, N.: Coupled chemistry-climate model simulation for the period 1980 to 2020: ozone depletion and the start of ozone recovery, Q. J. Roy. Meteor. Soc., 129, 3225–3249, 2003.

Austin, J. and Wilson, R. J.: Ensemble simulations of the decline and recovery of stratospheric ozone, J. Geophys. Res., 111, D16314, doi:10.1029/2005JD006907, 2006.

Austin, J., Wilson, R. J., Li, F., and Vömel, H.: Evolution of water vapor concentrations and stratospheric age of air in coupled chemistry-climate model simulations, J. Atmos. Sci., 64, 905–921, 2007.

Beagley, S. R., de Grandpré, J., Koshyk, J., McFarlane, N. A., and Shepherd, T. G.: Radiative-dynamical climatology of the first-generation Canadian Middle Atmosphere Model, Atmos. Ocean, 35, 293–331, 1997.

Birner, T., Sankey, D., and Shepherd, T. G.: The tropopause inversion layer in models and analyses, Geophys. Res. Lett., 33, L14804, doi:10.1029/2006GL026 549, 2006.

Bloom, S., da Silva, A., Dee, D., Bosilovich, M., Chern, J.-D., Pawson, S., Schubert, S., Sienkiewicz, M., Stajner, I., Tan, W.-W., and Wu, M.-L.: Documentation and Validation of the Goddard Earth Observing System (GEOS) Data Assimilation System – Version 4, Tech. Rep. Technical Report Series on Global Modeling and Data Assimilation 104606, 26, 165 pp., NASA, 2005.

Bony, S., Colman, R., and Kattsov, V. M.: How Well Do We Understand and Evaluate Climate Change Feedback Processes, J. Climate, 19, 3445–3482, 2006.

Butchart, N., Scaife, A. A., Bourqui, M., Grandpré, J., Hare, S. H. E., Kettleborough, J., Langematz, U., Manzini, E., Sassi, F., Shibata, K., Shindell, D., and Sigmond, M.: Simulations of anthropogenic change in the strength of the Brewer-Dobson circulation, Clim. Dynam., 27, 727–741, doi:10.1007/s00382-006-0162-4, 2006.

Dameris, M., Matthes, S., Deckert, R., Grewe, V., and Ponater, M.: Solar cycle effect delays onset of ozone recovery, Geophys. Res. Lett., 33, L03806, doi:10.1029/2005GL024741, 2006.

Dameris, M., Grewe, V., Ponater, M., Deckert, R., Eyring, V., Mager, F., Matthes, S., Schnadt, C., Stenke, A., Steil, B., Brühl, C., and Giorgetta, M. A.: Long-term changes and variability in a transient simulation with a chemistry-climate model employing realistic forcing, Atmos. Chem. Phys., 5, 2121–2145, 2005, http://www.atmos-chem-phys.net/5/2121/2005/.

de Grandpré, J., Beagley, S. R., Fomichev, V. I., Griffioen, E., McConnell, J. C., Medvedev, A. S., and Shepherd, T. G.: Ozone climatology using interactive chemistry: results from the Canadian Middle Atmosphere Model, J. Geophys. Res., 105, 26475–26491, 2000.

Efron, B. and Tibshirani, R. J.: An introduction to the Bootstrap, vol. 57 of Monographs on Statistics and Applied Probability, Chapman and Hall, New York, 436 pp., 1993.

Egorova, T., Rozanov, E., Zubov, V., Manzini, E., Schmutz, W., and Peter, T.: Chemistry-climate model SOCOL: a validation of the present-day climatology, Atmos. Chem. Phys., 5, 1557–1576, 2005, http://www.atmos-chem-phys.net/5/1557/2005/.

Eyring, V., Butchart, N., and Waugh, D. W.: Assessment of temperature, trace species, and ozone in chemistry-climate model simulations of the recent past, J. Geophys. Res., 111, D22308, doi:10.1029/2006JD007327, 2006.

Eyring, V., Waugh, D. W., and Bodeker, G. E.: Multi-model projections of stratospheric ozone in the 21st century, J. Geophys. Res., 112, D16303, doi:10.1029/2006JD008332, 2007.

Forster, P. M. d. F. and Shine, K. P.: Assessing the climate impact of trends in stratospheric water vapor, Geophys. Res. Lett., 29, 1086, doi:10.1029/2001GL013909, 2002.

Fueglistaler, S. and Haynes, P. H.: Control of interannual and longer-term variability of stratospheric water vapor, J. Geophys. Res., 110, D24108, doi:10.1029/2005JD006019, 2005.

Garcia, R. R., Marsh, D. R., Kinnison, D. E., Boville, B. A., and Sassi, F.: Simulation of secular trends in the middle atmosphere, 1950–2003, J. Geophys. Res., 112, D09301, doi:10.1029/2006JD007485, 2007.

Gettelman, A. and Birner, T.: Insights on Tropical Tropopause Layer Processes using Global Models, J. Geophys. Res., 112, D23104, doi:10.1029/2007JD008945, 2007.

Gettelman, A. and Forster, P. M. F.: A Climatology of the Tropical Tropopause Layer, J. Met. Soc. Jpn., 80, 911–924, 2002.

Gettelman, A. and Kinnison, D. E.: The global impact of supersaturation in a coupled chemistry-climate model, Atmos. Chem. Phys., 7, 1629–1643, 2007, http://www.atmos-chem-phys.net/7/1629/2007/.

Gettelman, A., Randel, W. J., Massie, S., Wu, F., Read, W. G., and Russell III, J. M.: El-Niño as a natural experiment for studying the tropical tropopause region, J. Climate, 14, 3375–3392, 2001.

Gettelman, A., Randel, W. J., Wu, F., and Massie, S. T.: Transport of water vapor in the tropical tropopause layer, Geophys. Res. Lett., 29, 1009, doi:10.1029/2001GL013818, 2002.

Holton, J. R. and Gettelman, A.: Horizontal transport and dehydration in the stratosphere, Geophys. Res. Lett., 28, 2799–2802, 2001.

IPCC: Special Report on Emission Scenarios, Cambridge University Press, New York, 612 pp., 2000.

Johns, T. C., Durman, C. F., and Banks, H. T.: The new Hadley Centre climate model Had-GEM1: Evaluation of coupled simulations, J. Climate, 19, 1327–1353, 2006.

Jourdain, L., Bekki, S., Lott, F., and Lefevre, F.: The coupled chemistry-climate model LMDz-REPROBUS: description and evaluation of a transient simulation of the period 1980–1999, Ann. Geophys., 26, 1391–1413, 2008, http://www.ann-geophys.net/26/1391/2008/.

Kalnay, E., Kanamitsu, M., Kistler, R., Collins, W., Deaven, D., Gandin, L., Iredell, M., Saha, S., White, C., Woollen, J., Zhu, Y., Chelliah, M., Ebisuzaki, W., Higgins, W., Janowiak, J., Mo, K. C., Ropelewski, C., Wang, J., Leetmaa, A., Reynolds, R., Jenne, P., and Joseph, D.: The NCEP/NCAR 40-year reanalysis project, B. Am. Meteorol. Soc., 77, 437–471, 1996.

Kurokawa, J., Akiyoshi, H., Nagashima, T., Masunaga, H., Nakajima, T., Takahashi, M., and Nakane, H.: Effects of atmospheric sphericity on stratospheric chemistry and dynamics over Antarctica, J. Geophys. Res., 110, D21305, doi:10.1029/2005JD005798, 2005.

Lott, F. L., Hourdin, F., and Levan, P.: The stratospheric version of LMDz: Dynamical Climatologies, Arctic Oscillation and Impact on the Surface Climate, Clim. Dynam., 25, 851–868, doi:10.1007/s00382-005-0064-x, 2005.

Manzini, E., Steil, B., Brühl, C., Giorgetta, M. A., and Krüger, K.: A new interactive chemistry climate model. 2: Sensitivity of the middle atmosphere to ozone depletion and increase in greenhouse gases: implications for recent stratospheric cooling, J. Geophys. Res., 108(D14), 4429, doi:10.1029/2002JD002977, 2003.

Meehl, G. A., Washington, W. M., Santer, B. D., Collins, W. D., Arblaster, J. M., Hu, A., Lawrence, D. M., Teng, H., Buja, L. E., and Strand, W. G.: Climate Change Projections for the Twenty-First Century and Climate Change Commitment in CCSM3, J. Climate, 19, 2597–2616, 2006.

Pawson, S. and Fiorino, M.: A comparison of reanalyses in the tropical stratosphere, Part 3, Inclusion of the pre-satellite data era, Clim. Dynam., 15, 241–250, 1999.

Pitari, G., Mancini, E., Rizzi, V., and Shindell, D.: Impact of future climate and emission changes on stratospheric aerosols and ozone, J. Atmos. Sci., 59, 414–440, 2002.

Randel, W. J., Wu, F., Oltmans, S. J., Rosenlof, K., and Nedoluha, G. E.: Interannual changes of stratospheric water vapor and correllations with tropical tropopause temperatures, J. Atmos. Sci., 61, 2133–2148, 2004.

Randel, W. J., Wu, F., Vomel, H., Nedoluha, G. E., and Forster, P. F.: Decreases in stratospheric water vapor since 2001: links to changes in the tropical tropopause and the Brewer-Dobson Circulation, J. Geophys. Res., 111, D12312, doi:10.1029/2005JD006744, 2006.

Rozanov, E., Schraner, M., Schnadt, C., Egorova, T., Wild, M., Ohmura, A., Zubov, V., Schmutz, W., and Peter, T.: Assessment of the ozone and temperature variability during 1979–1993 with the chemistry-climate model SOCOL, Adv. Space. Res., 35, 1375–1384, 2005.

Santer, B. D., Wehner, M. F., Wigley, T. M. L., Sausen, R., Meehl, G. A., Taylor, K. E., Ammann, C., Arblaster, J., Washington, W. M., Boyle, J. S., and Brüggemann, W.: Contributions of Anthropogenic and Natural Forcing to Recent Tropopause Height Changes, Science, 301, 479–483, doi:10.1126/science.1084123, 2003.

Santer, B. D., Wigley, T. M. L., and Mears, C.: Amplification of Surface Temperature Trends and Variability in the Tropical Atmosphere, Science, 309, 1551–1556, doi:10.1126/science.1114867, 2005.

Seidel, D. J. and Randel, W. J.: Variability and trends in the global tropopause estimated from Radiosonde data, J. Geophys. Res., 111, D21101, doi:10.1029/2006JD007363, 2006.

Seidel, D. J., Ross, R. J., Angell, J. K., and Reid, G. C.: Climatological characteristics of the tropical tropopause as revealed by Radiosondes, J. Geophys. Res., 106, 7857–7878, 2001.

Seidel, D. J., Fu, Q., Randel, W. J., and Reichler, T.: Widening of the tropical belt in a changing climate, Naure Geosci., 1, 21–24, doi:10.1038/ngeo.2007.38, 2008.

Shibata, K. and Deushi, M.: Partitioning between resolved wave forcing and unresolved gravity wave forcing to the quasi-biennial oscillation as revealed with a coupled chemistry-climate model, Geophys. Res. Lett., 32, L12820, doi:10.1029/2005GL022885, 2005.

Shibata, K., Deushi, M., Sekiyama, T. T., and Yoshimura, H.: Development of an MRI chemical transport model for the study of stratospheric chemistry, Papers in Met. and Geophys., 55, 75–119, 2005.

Solomon, S., Qin, D., Manning, M., Chen, Z., Marquis, M., Averyt, K. B., Tignor, M., and Miller, H. L.: Climate Change 2007 – The Physical Science Basis: Working Group I Contribution to the Fourth Assessment Report of the IPCC (Climate Change 2007), Cambridge University Press, Cambridge, UK, 1008 pp., 2007.

Son, S. W., Polvani, L. M., Waugh, D. W., Birner, T., Akiyoshi, H., Garcia, R. R., Gettelman, A., Plummer, D. A., and Rozanov, E.: The impact of stratospheric ozone recovery on tropopause height trends, J. Climate, 2008.

Steil, B., Brühl, C., Manzini, E., Crutzen, P. J., Lelieveld, J., Rasch, P. J., Roeckner, E., and Krüger, K.: A new interactive chemistry climate model. 1: Present day climatology and interannual variability of the middle atmosphere using the model and 9 years of HALOE/UARS data, J. Geophys. Res., 108, 4290, doi:10.1029/2002JD002971, 2003.

Stephens, G. L.: Cloud Feedbacks in the Climate System: A Critical Review, J. Climate, 18, 237–273, 2005.

Stolarski, R. S., Douglass, A. R., Steenrod, S., and Pawson, S.: Trends in Stratospheric Ozone: Lessons Learned from a 3D Chemical Transport Model, J. Atmos. Sci., 63, 1028–1041, 2006.

Struthers, H., Kreher, K., Austin, J., Schofield, R., Bodeker, G., Johnston, P., Shiona, H., and Thomas, A.: Past and future simulations of NO_2 from a coupled chemistry-climate model in comparison with observations, Atmos. Chem. Phys., 4, 2227–2239, 2004, http://www.atmos-chem-phys.net/4/2227/2004/.

Thuburn, J. and Craig, G. C.: On the temperature structure of the tropical substratosphere, J. Geophys. Res., 107, 4017, doi:10.1029/2001JD000448, 2002.

Tian, W. and Chipperfield, M. P.: A new coupled chemistryclimate model for the stratosphere: The importance of coupling for future O3-climate predictions, Q. J. Roy. Meteor. Soc., 131, 281–304, 2005.

Uppala, S., Kallberg, P., Simmons, A., Andrae, U., da Costa Bechtold, V., Fiorino, M., Gibson, J., Haseler, J., Hernandez, A., Kelly, G., Li, X., Onogi, K., Saarinen, S., Sokka, N., Allan, R., Andersson, E., Arpe, K., Balmaseda, M., Beljaars, A., van de Berg, L., Bidlot, J., Bormann, N., Caires, S., Chevallier, F., Dethof, A., Dragosavac, M., Fisher, M., Fuentes, M., Hagemann, S., Holm, E., Hoskins, B., Isaksen, L., Janssen, P., Jenne, R., McNally, A., Mahfouf, J.-F., Morcrette, J.-J., Rayner, N., Saunders, R., Simon, P., Sterl, A., Trenberth, K., Untch, A., Vasiljevic, D., Viterbo, P., and Woollen, J.: The ERA-40 re-analysis, Q. J. Roy. Meteor. Soc., 131, 2961–3012, 2005.

WMO (World Meteorological Organization), Scientific Assessment of Ozone Depletion: 2002, Global Ozone Research and Monitoring Project – Report No. 47, 498 pp., Geneva, Switzerland, 2003.

WMO (World Meteorological Organization), Scientific Assessment of Ozone Depletion: 2006, Global Ozone Research and Monitoring Project – Report No. 50, 572 pp., Geneva, Switzerland, 2007.

Yin, J. H.: A consistent poleward shift of the storm tracks in simulations of 21st century climate, Geophys. Res. Lett., 32, L18701, doi:10.1029/2005GL023684, 2005.